Piezo2 mediates ultrasonic hearing via cochlear outer hair cells in mice

Jie Li[1,2,11], Shuang Liu[1,2,11], Chenmeng Song[1,2,11], Qun Hu[1,2,11], Zhikai Zhao[1,2,11], Tuantuan Deng[2,3], Linzhi Zou[1,2], Shufeng Wang[1,2], Jiaofeng Chen[1,2], Lian Liu[1,2], Hanqing Hou[1,2], Kexin Yuan[2,4], Hairong Zheng[5], Zhiyong Liu[6], Xiaowei Chen[7,8], Wenzhi Sun[9,10], Bailong Xiao[2,3], Wei Xiong[1,2,*]

[1]School of Life Sciences, Tsinghua University, Beijing 100084, China

[2]IDG/McGovern Institute for Brain Research at Tsinghua University, Tsinghua University, Beijing 100084, China

[3]School of Pharmaceutical Sciences, Tsinghua-Peking Joint Center for Life Sciences, Tsinghua University, Beijing 100084, China

[4]Department of Biomedical Engineering, School of Medicine, Tsinghua University, Beijing 100084, China

[5]Paul C. Lauterbur Research Center for Biomedical Imaging, Shenzhen Key Laboratory for MRI, Shenzhen Institutes of Advanced Technology, Chinese Academy of Sciences, Shenzhen, 518005, China

[6]Institute of Neuroscience, CAS Center for Excellence in Brain Science and Intelligence Technology, Shanghai Institutes for Biological Sciences, Chinese Academy of Sciences, Shanghai 200031, China

[7]Brain Research Center and State Key Laboratory of Trauma, Burns, and Combined Injury, Third Military Medical University, Chongqing, China.

[8]CAS Center for Excellence in Brain Science and Intelligence Technology, Shanghai Institutes for Biological Sciences, Chinese Academy of Sciences, Shanghai, China.

[9]Chinese Institute for Brain Research, Beijing 102206, China

[10]School of Basic Medical Sciences, Capital Medical University, Beijing 100069, China

[11]These authors contributed equally

*Corresponding Author

ABSTRACT

Ultrasonic hearing is exploited for hunting and navigation as in echolocation by microbats and bottleneck dolphins and for social communication like ultrasonic vocalization by mice and rats. However, the molecular basis for ultrasonic hearing is not known yet. Here we show that knockout of the mechanosensitive ion channel Piezo2 in cochlear outer hair cells disrupts the USH but not the low-frequency hearing in mice, as shown by audiometry, acoustically-associative learning behavior, and pup-retrieval behavior. Together, our study demonstrates that Piezo2 is molecularly essential for ultrasonic vocalization based communication in mouse social lives.

INTRODUCTION

Some animals use ultrasonic hearing (USH) and vocalization to communicate and navigate (*1*). For example, mice vocalize at frequencies > 25 kHz and with intensities from 60 dB SPL to 100 dB SPL during certain social behaviors, including pup retrieval, male-male encounter, and male-female courtship (*2-4*), which is critical for their survival and generation. Study on animal models, including mice, bats, cats, and Guinea pigs, has provided neurophysiological insights into USH (*5-9*) but lacked precise molecule identity and cell-type definition concerning ultrasonic transduction. It cannot even be excluded whether the vestibular input participates in USH, as vestibular evoked myogenic potentials recorded from patients with profound deafness suggested that certain hearing sensitivity is not from cochlear origin (*10, 11*). Together, the molecular and cellular mechanisms underlying USH is largely unknown and is often thought to share the same mechanisms for audible sound transduction that has been well recognized (*12, 13*).

It was recently reported that the mechanosensitive ion channel Piezo2 plays critical roles in

the somatosensory system, including gentle touch, itch, tactile pain, proprioception, breath, and blood pressure (*14*). Structural and functional analysis of Piezo2 has shown that it can respond to different forms of mechanical stimuli, such as indentation and stretching (*15, 16*). Interestingly, Piezo2 was found to express at the apical surface of cochlear hair cells, mainly outer hair cells (OHCs), and mediates a stretch-activated current in neonatal mice. However the current gradually reduces when ageing and finally disappears after onset of hearing (12-14 days) (*17-19*), and knockout of Piezo2 only slightly affects hearing from 8 kHz to 20 kHz in adult mice as tested by the auditory brainstem response (ABR) recording (*18*). Thus, the virtual physiological role of Piezo2 in hearing is still elusive.

In this study, we studied the role of Piezo2 in USH based a variety of knockout (KO) and conditional knockout (cKO) mouse lines, by newly developed approaches, including ultrasonic ABR, behavior tests, and *ex vivo* cochlear imaging assays. We found that Piezo2 expressing in the OHCs is essential for USH in mice.

RESULTS

The mechanosensitive channel Piezo2 is required for ultrasound hearing

To characterize whether Piezo2 participates USH, we initially developed the basic ABR to expand its detection stability and sensitivity to ultrasonic frequencies in mice (Fig. 1A), by connecting the electrode to a microscrew nailed at the skull bone positioned posterior to Bregma sutures (-7 mm AP, 0 mm ML) (fig. S1 and Methods), named as nail ABR (nABR) recording. Since the C57BL/6 (B6) mice exhibit progressive hearing loss late in life (> 7 months) (*20, 21*), the mice at age around 1 month were used to ensure their USH sensitivity, unless otherwise stated. Because genetically modified mice with mixed genetic background would be used in this study, we made comparison of nABR sensitivity between the B6 mice and the CBA/J (CBA) mice (Fig. 1B), as it has been shown that the CBA mice have better hearing

sensitivity than that of B6 mice according to the auditory nerve recordings (*22*) and ABR recordings (*23*). The similar nABR thresholds were observed in the two groups of the mice upon hearing ultrasonic frequencies (Fig. 1B), indicating the nABR recording is feasible to evaluate USH in the B6 mice or the mice with mixed genetic background, at least at the age of one month. The nABR waveforms induced by ultrasonic frequencies were distinguishable by justifying the thresholds although they were not as strong as those by low frequencies (Fig. 1C), implying less efficient USH transduction at the cochlear level because the ABR waves reflect signals from the auditory nerves that innervate the cochlear hair cells, and their ascending auditory pathways (*24*). The 54-kHz nABR signals suddenly show peaks as sensitive as the 16-kHz signals (Fig. 1C), which is consistent to previous observation achieved by behavioral test (*25*) and auditory nerve recordings (*22*). It was not due to distortions delivered by the speaker at high intensities, since the measured ultrasonic pure-tone output was very condensed even at 90 dB SPL (fig. S1D). We next checked the nABR performance in the inner-ear targeted *Piezo2*-cKO mice by crossing the $Piezo2^{f/f}$ mice with either the $Pax2^{Cre}$ mice (*18, 26*) or the $Atoh1^{Cre}$ mice (*27*), as the *Piezo2* pan-knockout mice are embryonic-lethal (*28*). The nABR recordings revealed that these *Piezo2*-cKO mice had reduced sensitivity of USH specifically (32-80 kHz) but not to low-frequency hearing (LFH, 4-16 kHz), with their littermates used as control (Fig. 1, D and E). The control $Pax2^{Cre}$ mice have similar nABR threshold as the B6 mice and the CBA mice (Fig. 1, B and E), which is slightly different from the previous observation that showed reduced ABR in the 2-month $Pax2^{Cre}$ mice (*18*), probably due to difference from the ABR configuration and mouse ages. These data demonstrate that Piezo2 is required for USH.

Ultrasonically-associative freezing behavior is disrupted in *Piezo2*-knockout mice

Next, we wondered whether Piezo2-mediated ultrasound sensitivity is required for learned behavior in animals. The hearing response of the *Piezo2*-cKO mice was examined by a fear conditioning test (Fig. 2A). The ultrasonic 63-kHz stimulatory cue was used because it is in the

steady state within the range of applied ultrasonic frequencies (Fig. 1E) and because mice are known to use this frequency in social communication (*1*). Comparison of freezing responses to the 90-dB 16-kHz cue for the control *Pax2*^{Cre} mice and *Piezo2*$^{f/f}$ mice with the *Pax2*^{Cre}*;Piezo2*$^{f/f}$ and *Atoh1*^{Cre}*;Piezo2*$^{f/f}$ cKO mice showed that all genotypes retained their LFH-associated freezing behavior, as shown in locomotion (Fig. 2B) and calculated velocity over time (Fig. 2C). Because the locomotion condition was variable from mouse to mouse, we assessed their fear conditioning by monitoring their averaged velocity before and after the cue (Fig. 2, D and E), which was further calculated to freezing index values (Fig. 2, F and G, and Methods). These results reveal that the *Piezo2*-cKO mice did not exhibit triggered freezing behavior upon hearing the 63-kHz cue, while this acoustically learned behavior was preserved in the control mice.

Piezo2-knockout mother mice lack pup-call triggered retrieval behavior

We further examined whether Piezo2 mediates the ultrasonic communication in animal lives by using a pup-retrieval paradigm (*3*) (Fig. 3A and Methods) because the frequencies of pup calls cover the ultrasound range (50 – 100 kHz) (fig. S3A). The *Piezo2*-cKO mother mice could retrieve their isolated pups as the control when in a natural circumstance (fig. S3, B to D). To test the influence from USH, we played pre-recorded pup calls back to the mother mouse through a tube in the test arena and evaluated their exploring behavior (Fig. 3A). The footage showed that upon audio playback of the pre-recorded calls from her pups, the control mother mouse moved more frequently to the tube with the call playback (Fig. 3B). Remarkably, such directed locomotion toward the source of pup calls was lost in the *Pax2*^{Cre}*;Piezo2*$^{f/f}$ cKO mother mouse (Fig. 3B). Quantitative analysis of locomotion revealed that the control mother mice, but not the cKO mice, had a strong preference to explore in the tube with playback (Fig. 3C) and in the arena close to the playback (Fig. 3D). The pup-call preference could also be seen by counting the number of entries into the tube in control mice, but not in *Piezo2*-cKO mice (Fig. 3E). These results demonstrate that Piezo2 is required for the social behavior that recruits

ultrasonic hearing and communication.

Hair-cell mechanotransduction is required for ultrasonic hearing

Next we wondered which type of cell in the inner ear supports Piezo2's function for USH. Given their integral role in hearing, the hair cells were examined first. CDH23 is the component of the tip link (*29, 30*) to gate the mechano-electrical transduction (MET) channel that TMC1 was recently considered as the channel pore for MET in hair cells (*31*), while vGlut3 is highly expressed on the vesicular membrane of cochlear inner hair cells (IHCs) that transports glutamate into synaptic vesicles (*32*). We checked ultrasonic response in *Cdh23*-null, *Tmc1*-KO and *vGlut3*-KO mice, as all three mouse lines are deaf in LFH due to dysfunctions in either signal input (MET) or signal output (neurotransmission) of the hair cells. Both low-frequency and high-frequency nABRs were completely lost in these mice, in contrast to 4-80 kHz cues elicited responses in control WT mice (Fig. 4A), which however is not yet to define the cochlear hair cells as the target cells to ultrasound because *Cdh23*, *Tmc1*, and *vGlut3* are expressed in vestibular hair cells too. We then examine the ultrasonic response directly in cochlear hair cells by delivering ultrasound of 80 kHz, a frequency within the range of the physiological hearing of mice, via a custom *ex vivo* ultrasonic stimulation stage (fig. S4, A to C, and Methods). Because it is difficult to obtain the organ of Corti from mice after hearing onset because the cochlea has been embedded into the bony capsule of the inner ear, we introduced the hemicochlear preparation (*33, 34*) that preserves most of the elements of the cochlea and is also accessible for microscopic observation. Because the electrophysiological recording of the hair cells was always destroyed by the ultrasonic stimulation, we turned to use Ca^{2+} imaging for monitoring the ultrasonically-evoked activity (Fig. 4, B and C). The hemicochlear preparation was loaded with Fluo-8 AM, a sensitive Ca^{2+} dye, and OHCs were the major cells with Ca^{2+} dye uptake (Fig. 4C). The ultrasonic stimulation elicited Ca^{2+} waves in OHCs of WT hemicochleae could be blocked

when perfusing the 0.1 mM Ca^{2+} solution, and the loaded OHCs showed intracellular Ca^{2+} release when applying ATP (100 μM) (fig. S4, D and E), prompting OHC is a ultrasound-responsive cell. The ultrasonic Ca^{2+} response was hardly seen in the *Tmc1*-KO OHCs or in the WT OHCs blocked by the MET channel blocker dihydrostreptomycin (DHS, 100 μM) (Fig. 4, D to F). The hemicochlear imaging experiment further revealed that the ultrasonic stimulation could elicit Ca^{2+} response in OHCs of the control *Piezo2*$^{f/f}$ mice, but hardly in OHCs when genetically removing *Piezo2* (Fig. 4G). Lack of USH is not due to loss of the "high-frequency" hair cells in the *Piezo2*-cKO mice, as their hair cells at the very basal cochlear coil were well conserved and normal in morphology (fig. S5). However, we did not observe any response in the HEK293T cells expressing Piezo2 or Piezo2 and Tmc1 when using the 80-kHz ultrasonic stimulation similar to the hemicochlear imaging (Fig. 4, H and I), although the HEK293T cells expressing Piezo2 were mechanosensitive (fig. S6). These results indicate that Piezo2 coordinates with the MET channel to fulfil the ultrasonic transduction.

Mice lack ultrasonic hearing when deleting Piezo2 in outer hair cells

To examine which type of hair cell, OHC or IHC, is the target cells for USH, we initially used immunostaining to define Piezo2's expression. Piezo2 was mainly detected at the apical surfaces of cochlear OHCs at P5 (fig. S7A) and *Piezo2* promoter drives mCherry expression as observed in 1-month *Piezo2*^{Cre}*;H2B-mCherry* mice (fig. S7, B to E), as previously reported (*18*). We further examined the USH-associative freezing behavior in mice when deleting Piezo2 in OHCs. Then *Prestin*^{CreER} mice was introduced to generate OHC-specific *Piezo2*-cKO mice as *Prestin* only expresses in OHCs, and the *vGlut3*^{CreER}*;Piezo2*$^{f/f}$ mice were used to check Piezo2's role in IHCs, from which USH-associated freezing behavior in the mice were compared before and after the tamoxifen injection (Fig. 5A). The induced *Prestin*^{CreER}*;Piezo2*$^{f/f}$ cKO mice showed freezing behavior with the low-frequency stimulation but not the ultrasonic cue (Fig. 5, A and B).

On the contrary, *vGlut3^{CreER};Piezo2$^{f/f}$* mice did not show deficit of USH-associated freezing (Fig. 5, C and D), which excludes a possible role of IHCs to support Piezo2's function in ultrasound detection. The *CreER*-induced expression was OHC and IHC -specific, as indicated by mCherry signal in the *Prestin^{CreER};H2B-mCherry* mice and the *vGlut3^{CreER};H2B-mCherry* mice (fig. S8). Together, these data confirm that the cochlear OHC expression of Piezo2 is required for USH.

DISCUSSION

Piezo2's mechanic properties likely support its role for OHCs in ultrasound transduction. Piezo2 is a mechanosensitive channel that homotrimerizes to form a gigantic (~0.9 Mega-Dalton) three-bladed propeller-like structure comprising 114 transmembrane (TM) domains (38 TM per protomer), making it a unique membrane protein with the largest number of TMs (*15*). Strikingly, the three unusual non-planar TM Blades are curved into a nano-bowl shape of 28 nm-diameter and 10 nm-depth, which might deform the residing membrane to produce a mid-plane nano-bowl surface area of 700 nm^2 and a projected in-plane area of 450 nm^2. On the basis of the unique nano-bowl shape of the Piezo channel-membrane system, flattening the non-planar TM-Blades might produce a maximal change of the projection area of ~250 nm^2, which might provide the energy to gate the channel (*15*). The curved configuration of the Piezo channels (Piezo1 and Piezo2) might further deform the membrane shape outside of the perimeter of the channel into a large, curved 'membrane footprint' (*35*), which might further amplify the mechanosensitivity of the Piezo channels. Such 'membrane-dome' (*36*) and 'membrane footprint' (*35*) mechanisms have been proposed to account for the exquisite mechanosensitivity of Piezo channels in response to various mechanical stimulation including poking and stretch, which may underlie the Piezo1's response to the non-physiological ultrasonic stimulation (0.5 MHz) (*37*). However, removal of either Piezo2 or Tmc1 destroyed ultrasonic transduction (80 kHz) in cochlear hair cells (Fig. 4), suggesting a more complicated mechanism to transduce

ultrasonic frequencies. To detect physiological ultrasound, Piezo2 may locate at the apical surface of the hair cell, where the stereocilia root and a place least influenced by membrane low-pass filtering, and coordinate with the MET complex to transduce the ultrasonic vibration, suggested by the evidence that the mice lose ultrasound sensitivity after removing key MET components of hair cells, e.g. CDH23 or TMC1 (Fig. 5, A to F). It may explain why the HEK293T cells expressing Piezo2 and/or TMC1 failed to show ultrasonic response (Fig. 5, H and J).

Interestingly, the cochlear OHC, not the IHC, is the target cell to support Piezo2 to sense ultrasound (Fig. 4 and 5), by which the animal gains extended spectral sensitivity from 16 kHz toward ultrasonic frequencies (Fig. 1E). The IHC may simply output the encoded ultrasound information from the organ of Corti, coinciding with the evidence that the *vGlut3*-KO mice completely lack ultrasonic ABRs (Fig. 4A) and the induced *vGlut3*^{CreER}*;Piezo2*$^{f/f}$ mice have normal ultrasonic freezing (Fig. 5, D and F). With Piezo2, the OHCs may use a mechanism like ciliary motility to transfer the ultrasonic vibration to the IHCs through the tectorial membrane.

In summary, we discovered that Piezo2 in OHCs plays an indispensable role in the high-frequency USH, indicating an alternative auditory transduction mechanism in mammals. It would be intriguing to study Piezo2's role in USH from other species, e.g. bats and whales. Given that both USH and LFH critically depend on cochlear OHCs but may use different neural mechanisms, it will be interesting to investigate the responding pattern to ultrasonic frequencies in cochlea, i.e. whether it also follows place-code principle, which can be probed by *in vivo* cochlear imaging, an approach to be developed. Moreover, our study lays the foundation to further address whether USH and LFH use distinct structural and functional circuits in brain regions along the ascending auditory pathways.

MATERIALS AND METHODS

Mouse strains and animal care

In this study, *Cdh23*$^{v-2j}$ mice (Stock No. 002552, named *Cdh23*-null in this study) , B6.129-*Tmc1*$^{tm1.1Ajg}$/J mice (Stock No. 019146, named *Tmc1*-knockout in this study) , and *Rosa26 LSL H2B mCherry* mice (Stock No. 023139, named *H2B-mCherry* in this study) were from the Jackson Laboratory (Bar Harbor, ME); *vGlut3* knockout mice and *Prestin* knockout mice were generated by CRISPR/Cas9-mediated base editing ; *Pax2-Cre* mouse line (named *Pax2*^{Cre} in this study) was generated by Dr. Andrew Groves and *Atoh1-Cre* mice (named *Atoh1*^{Cre} in this study) were kindly from Dr. Lin Gan ; *Piezo2*$^{loxP/loxP}$ (named *Piezo2*$^{f/f}$ in this study) and *Piezo2-GFP-IRES-Cre* (named *Piezo2-GFP* or *Piezo2*^{Cre} in this study) mice were gifts from Dr. Ardem Patapoutian at the Scripps Research Institute ; Prestin-CreER^{T2} (*Prestin*^{CreER} in this study) mouse line was a gift from Dr. Jian Zuo ; *vGlut3-P2A-iCreER* knockin mouse strain was generated as described and here named as *vGlut3*^{CreER} mouse. All the mice were crossed in mixed genetic background and their littermates were selected as control. Tamoxifen (Sigma, 20mg/mL in corn oil) was injected into the mice with *CreER* background intraperitoneally (i.p.) at age of 1 month, with a dose of 9mg/40g (tamoxifen/body weight). The *Prestin*^{CreER};*Piezo2*$^{f/f}$ mice were injected once a day for 2 days and the *vGlut3*^{CreER};*Piezo2*$^{f/f}$ mice were injected once a day for 4 days. The experimental procedures on mice were approved by the Institutional Animal Care and Use Committee of Tsinghua University.

Histology

Immunostaining

The mice were selected for immunostaining at indicated ages. After anesthesia, the mouse was sacrificed by decapitation and the inner ears were dissected from the temporal bone. Then the inner ears were fixed by 4% Paraformaldehyde (PFA) (DF0135, Leagene, Anhui, China) in Phosphate Buffered Saline (PBS) for 1.5 hours at room temperature (RT, 20 - 25 °C). After fixation, the inner ears were washed with PBS for three times (10 min for each time), and then

were treated in EDTA decalcifying solution (pH 7.2, Cat. E1171, Solarbio, China) for 24 hours at RT followed by PBS washing. The cochlear coils were finely dissected from the inner ears in PBS and blocked in 0.5% PBST (PBS + 0.5% Triton X-100 (T8787, Sigma-Aldrich, St. Louis, MO)) solution with 4% BSA (A3059, Sigma-Aldrich, St. Louis, MO) at RT for 2 h. The cochlear tissues were then incubated in PBST solution with MYO7A antibody (1:1000, Cat.25-6790, Proteus Biosciences Inc., Ramona, CA) and 1% BSA overnight at 4 °C and washed with PBS for three times at RT. The tissues were incubated with secondary antibody (Invitrogen anti-Rabbit Alexa Fluor 647, 1:1000, A21244; Invitrogen Alexa Fluor 488 Phalloidin, 1:1000, Cat. A12379) and 1:1000 DAPI in PBST solution with 1%BSA at RT for 2 hours. Tissues were washed with PBS three times and mounted by ProLong Gold Antifade Mountant (Cat. P36930, Life Technology, Rockville, MD). The photos of fluorescent immunostaining pattern were collected by a Spinning Disk confocal microscope (Ultraview VOX, PerkinElmer, Waltham, MA). The whole-view photos of the cochlear tissues were stitched by Imaris software (version 9.3.1, Bitplane, Oxford instruments, Abingdon, England). The immunostaining procedure of cochlear tissues from *Piezo2-GFP* mice was slightly changed based on the protocol above. For fixation, the inner ears were perfused by 2% fresh PFA and incubated at RT for 30-45 min without shaking. For blocking, the cochlear tissues were treated in 0.5% PBST solution with 4% BSA at RT for 2 h with slow shaking. The primary antibody (Rabbit anti-GFP; 1:500, Cat. A-11122, ThermoFisher Scientific, Waltham, MA) was made in 0.5% PBST with 1% BSA. For and then washed 3 times. Then the cochlear tissues were incubated in the secondary antibody (Invitrogen anti-Rabbit Alexa Fluor 647, 1:1000, Cat.A21244; Invitrogen Alexa Fluor 568 Phalloidin, 1:1000, Cat. A12380) was made in 0.5% PBST solution. Each incubation was shaken slowly.

In situ hybridization

The temporal bones were dissected from mice at 1 month. The membranes of round window and oval window were removed and a hole was made at the apex of cochlea. The temporal

bone was perfused with 4% PFA (DF0135, Leagene, Anhui, China) through the apex hole and then was incubated in fresh 4% PFA fixative at 4°C overnight. After the post-fixation, the cochleae were decalcified by incubating at EDTA decalcification solution (E1171, Solarbio, China) at 4°C for 24hr. Then the cochlear tissues were dissected out and dehydrated in 20% sucrose solution (DD0052, Leagene, Anhui, China) for 30 min and in 30% sucrose solution (R00771, Leagene, Anhui, China) for 45 min at 4°C respectively. The tissues were incubated in O.C.T (4583, Tissue-Tek, Torrance, CA) at 4°C overnight before embedded at -20°C. The embedded tissues were sliced into 20-μm sections (CryoStarTM NX50, ThermoFisher Scientific, Waltham, MA) and baked at 60°C for 1 h. The *Piezo2* transcript detection was performed according to manufacturer's instructions using RNAscope detection kit (323100, ACDBio, Newark, CA) and probe of *Piezo2* (439971, ACDBio, Newark, CA) .

Hemicochlear imaging

Hemicochlear preparation

Mice at 1-month age were anesthetized and sacrificed, and then their cochleae were dissected out in the dissection solution. Immersed in the cutting solution, the cochlea was glued on a metal block and cut to 2 halves by a vibratome (VT1200S, Leica, Wetzlar, Germany).

Ultrasound generation and delivery

A customized 80-kHz ultrasound transducer with diameter of 27 mm was powered by a customized radio-frequency amplifier integrated with a high-frequency function generator. The 80-kHz transducer was chosen because its size is small enough to be assembled (the lower the frequency, the larger the size) and 80 kHz is a physiological frequency to mice. For calibration, a high-sensitivity hydrophone (Precision Acoustics, United Kingdom) was positioned directly above the vibration surface. Transducer outputs were calibrated in a tank filled with deionized, degassed water under free-field conditions. To stimulate hemicochlea, the transducer was

tightly fixed at the bottom of recording dish with ultrasound gel in between. The distance between the tissue and ultrasound transducer is less than 5 mm. For the 80-kHz ultrasonic stimulation, a single pulse of 100 ms was applied, with calibrated intensities at 8.91 W/cm^2 I_{SPTA}. The ultrasound energy received by the tissue preparation was stable and homogeneous, as shown by calibrated intensities covering the whole bottom of the recording dish (Supplementary Fig. 5).

Hemicochlear imaging

The hemicochlea was transferred into a recording dish, and glued on the bottom, and loaded with 25 μg/mL Fluo-8 AM (Invitrogen, Waltham, MA) in the recording solution. After 5-min incubation at RT in a dark box, the dye-loading solution was replaced by the dye-free recording solution. An upright microscope (BX51WI, Olympus, Tokyo, Japan) equipped with 60X water immersion objective (LUMPlanFL, Olympus, Tokyo, Japan) and an sCMOS camera (ORCA Flash 4.0, Hamamatsu, HAMAMATSU-SHI, Japan) was used for calcium imaging, controlled by MicroManager 1.6 software (*38*) with a configuration of 4x4 binning, 100-ms exposure time, and 2-s sampling interval. To keep the best performance of the hemicochlea preparations, the whole procedure from cutting to imaging was finished within 15 min. As control experiments, 0.1 mM Ca^{2+} (to keep tip link structure) perfusion abolished the ultrasonic stimulation evoked Ca^{2+} signal, and 100 μM ATP perfusion induced strong Ca^{2+} response (~20%), in the OHCs of the hemicochleae. The dissection/cutting/recording solution contained (in mM): 145 NaCl, 1.3 $CaCl_2$, 0.9 $MgCl_2$, 10 glucose, and 10 H-HEPES (pH 7.4).

Single-cell Ca^{2+} imaging

HEK293T cells were plated onto 8-mm round glass coverslips, which were coated with poly-D-lysine and placed in 48-well plates. 400 ng of plasmids were transiently transfected into

HEK293T cells using lipofectine 2000 (Life Technologies). GCaMP6 was expressed to monitor the Ca^{2+} response. After 24h transfection, the HEK293T cells were imaged for Ca^{2+} signals by an upright microscope (BX51WI, Olympus, Tokyo, Japan) equipped with 60X water immersion objective (LUMPlanFL, Olympus, Tokyo, Japan) and an sCMOS camera (ORCA Flash 4.0, Hamamatsu, HAMAMATSU-SHI, Japan), controlled by MicroManager 1.6 software (*38*) with 50-ms exposure time and 1-s sampling interval.

Nail auditory brainstem response (nABR)

Mice were anesthetized (i.p.) with 0.4% pentobarbital sodium in saline. Body temperature was maintained at 37°C by a heating pad during the whole experiment. After the skin on the vertex was removed, the skull was exposed and nailed with a stainless-steel screw (M1.4*2.5) but not puncturing the dura. The recording electrode was connected to the screw by a silver wire with a diameter of 0.1 mm. Other operations were similar to regular ABR procedure. The reference electrode and the ground electrode were inserted subcutaneously at the pinna and the groin respectively. The mice harboring a bone screw in Type-A implantation best-exhibited the ultrasonic responses (Supplementary Fig. 1), which was used in this study. The ABR data were collected by an RZ6 workstation controlled by a BioSig software (Tucker-Davis Technologies, Alachua, FL). Clicks and 4-16 kHz pure-tone bursts were generated by a TDT MF1 closed-field magnetic speaker while a TDT EC1 (Coupler Model) electrostatic speaker was used for generating high frequencies (32-80 kHz). Upon each acoustic stimulation with defined frequency and intensity level, the responses were sampled 512 times repeatedly and then averaged.

Behavior test

Acoustic cue associated freezing behavior

Male mice were used. The mouse locomotion in an operant box (cubic, 30*30*30 cm) or an activity box (cylindrical, diameter of 35 cm and height of 30 cm) was monitored by an infrared camera with an infrared light as the light source, which was performed in a sound proof chamber (Shengnuo, Shanghai, China). Each mouse was allowed to freely explore the operant box for 30 min before the sound-associated footshock training. During the training, an acoustic cue of 10 s containing 50 ms pure tone (16 kHz or 63 kHz) at 50 ms interval was played, and electrical shocks of 1 s at current magnitude of 0.6 mA was given to the mouse at the 5^{th} s and 10^{th} s. In the operant box, the electrical shocks were delivered by the metal grid floor powered by an electrical stimulator (YC-2, Chengdu Instrument Inc., Chengdu, China), and the acoustic cues were given by a free-field electrostatic speaker ES1 placed 15 cm above the floor and powered by an RZ6 workstation and a BioSig software (Tucker-Davis Technologies, Alachua, FL). The cue was given every 3 min and repeated for 10 times before the trained mouse was put back to the home cage. After 24 hours, the trained mouse was transferred in an activity box to test the freezing behavior. In the activity box, the same ES1 speaker was placed 15 cm above the chamber floor to generate the 16 kHz or 63 kHz acoustic cues of 10 s duration (identical to the training cues) and the cues were given at least 5 times during the test procedure. As calibrated, the sound intensity on the arena floor was from 70 dB SPL to 90 dB SPL that is in the range of mouse hearing threshold (Supplementary Fig. 2, A and B).

Pup retrieval behavior

The 2-3 month female mice that were nursing their neonatal pups (P3-5) were used. The pup-retrieval behavior of a mother mouse was monitored in a test box (cubic, 30*30*30 cm) housed in a sound proof chamber (Shengnuo, Shanghai, China). At the 2 diagonal corners of the lateral boards of the box, holes (5 cm in diameter) were opened (hole-edge to board-edge, 0.5 cm) and glued with tubes (5 cm in diameter and 10 cm in length). The ends of the tubes were covered by metal meshes to make the tubes impassable to mice but sound permeable (Fig. 6A). The

mother mouse was placed in the chamber for a 30-min habituation period. When the mother was removed from the housing cage, the calls of her pups were recorded for 5 min by an ultrasound microphone (UltraSoundGate 116H, Avisoft Bioacoustics, Glienicke, Germany) from the isolated pups. The mother mouse was allowed to freely explore the test box for 30 min before playing back pup calls with an ultrasound speaker (UltraSoundGate Player 116, Avisoft Bioacoustics, Glienicke, Germany) at one tube end. After the habituation period, the pup calls were played back for 5 min and the locomotion of the mother mouse was monitored.

Data analysis

General data handling

Each experiment contained at least 3 biological replicates. Data were managed and analyzed with Matlab 2014b (MathWorks, Natick, MA), MicroManager 1.6 software (*38*), Excel 2016 (Microsoft, Seattle, WA), Prism 6 (GraphPad Software, San Diego, CA), and Igor pro 6 (WaveMetrics, Lake Oswego, OR). All data are shown as mean ± SEM or SD, as indicated in the figure legends. We used two-tailed *t*-test for one-to-one comparison or one-way ANOVA for one-to-many comparison to determine statistical significance (*p<0.05, **p<0.01, ***p<0.001, ****p<0.0001). N numbers are indicated in the figures.

Animal tracing and locomotion evaluation

Videos of mouse locomotion in foot-shock and pup-retrieval test were analyzed by Matlab software and EthoVision XT software (v11.5, Noldus, Wageningen, Netherland). The center of mice was used to draw locomotion trace. To show the speed information, the locomotion trace was dotted every 0.5 s.

For footshock behavior analysis, the velocity of animal was calculated as position-coordinates' derivation versus time (cm/s). Due to variable locomotion activities among animals, the *Freezing Index* was calculated. The calculation formula of *Freezing Index* is:

$$Freezing\ Index = (V_{pre} - V_{post}) / (V_{pre} + V_{post})$$

Where V_{pre} indicates the mean value of velocity in 30 s before the stimulation, and V_{post} indicates the mean value of velocity in 30 s after the stimulation.

For pup-retrieval behavior analysis, the square floor of the test box was divided equally into four quadrants, as I, II, III, and IV respectively. Quadrant I connected the tube with a speaker but not playing the pup calls, and quadrant IV connected the tube with a speaker playing the pup calls. The total time that the mouse traveled in each quadrant was summarized and shown as a heat map. The numbers of mouse entries into each of the two tubes were counted, and the time that mouse stayed in the two tubes was calculated. The mouse position was determined as "in tube" if its body (not including the tail) completely moved into the tube. If half of the mouse body emerged out of the tube, it was regarded as "in quadrant".

Ca^{2+} data analysis

To extract fluorescence signals, we visually identified the regions of interest (ROIs) based on fluorescence intensity. To estimate fluorescence changes, the pixels in each specified ROI were averaged (F). Relative fluorescence changes, $\Delta F/F_0 = (F-F_0) / F_0$, were calculated as Ca^{2+} signals. The hemicochlear imaging data were analyzed offline by Micromanager software and Excel software as described . The ROI was drawn to cover each hair cell. The fluorescence intensity of ROI was normalized to its value in the frame right before the stimulation.

SUPPLEMENTARY MATERIALS

Supplementary Materials and Methods

Whole-cell electrophysiology

HEK293T cells were recorded using whole-cell patch-clamp as previously described (*39*). All experiments were performed at room temperature (20-25°C). Briefly, the coverslip with cultured

cells was transferred into a recording chamber with recording solution containing (in mM): 144 NaCl, 0.7 NaH_2PO_4, 5.8 KCl, 1.3 $CaCl_2$, 0.9 $MgCl_2$, 5.6 glucose, and 10 H-HEPES (pH 7.4). The cells were imaged under an upright microscope (BX51WI, Olympus, Tokyo, Japan) with a 60× water-immersion objective and an sCMOS camera (ORCA Flash4.0, Hamamatsu, Hamamatsu City, Japan) controlled by MicroManager 1.6 software (*38*). Patch pipettes were made from borosilicate glass capillaries (BF150-117-10, Sutter Instrument Co., Novato, CA) with a pipette puller (P-2000, Sutter) and polished on a microforge (MF-830, Narishige, Tokyo, Japan) to resistances of 4-6 MΩ. Intracellular solution contained (in mM): 140 KCl, 1 $MgCl_2$, 0.1 EGTA, 2 Mg-ATP, 0.3 Na-GTP, and 10 H-HEPES, pH 7.2). The cells were recorded with a patch-clamp amplifier with a holding potential of –70 mV (EPC 10 USB and Patchmaster software, HEKA Elektronik, Lambrecht/Pfalz, Germany). The liquid junction potential is not corrected in the data shown. As measured, the pipette with CsCl intracellular solution had a value of +4 mV in regular recording solution.

Mechanical stimulation utilized a fire-polished glass pipette (tip diameter 3–4 mm) positioned at an angel of 80 relative to the cell being recorded as described (*39*). The probe was displaced by a piezoelectric actuator (P-601.1SL, Physik Instrumente, Karlsruhe, Germany) and driven by a piezoelectric crystal microstage (E625 LVPZT Controller/Amplifier, Physik Instrumente, Karlsruhe, Germany). The probe velocity was 1 μm/ms during the upward and downward movement, and the stimulus was kept constant for 100 ms. A series of mechanical steps in 1 μm increments was applied every 5–10 s.

Supplementary Figures

Fig. S1. Recording of nail auditory brainstem response in mice.

Fig. S2. Recording of sound-associated freezing behavior of mice.

Fig. S3. Pup retrieval behavior is preserved in *Piezo2*-cKO mice as in wild-type mice.

Fig. S4. Recording of calcium response of cochlear hair cells to ultrasonic stimulation.

Fig. S5. The very basal hair cells are alive in *Piezo2*-cKO mice.

Fig. S6. Recording of mechanosensitive current in HEK293T cells expressing Piezo2.

Fig. S7. *Piezo2-Cre* expresses in cochlear hair cells.

Fig. S8. Cre-driven reporter in cochlear hair cells after tamoxifen treatment.

REFERENCE

1. S. L. Hopp, M. J. Owren, C. S. Evan, *Animal Acoustic Communication: Sound Analysis and Research Methods*. (Springer, 1998).
2. C. V. Portfors, D. J. Perkel, The role of ultrasonic vocalizations in mouse communication. *Curr Opin Neurobiol* **28**, 115-120 (2014).
3. A. Uematsu *et al.*, Maternal approaches to pup ultrasonic vocalizations produced by a nanocrystalline silicon thermo-acoustic emitter. *Brain Res* **1163**, 91-99 (2007).
4. S. R. Egnor, K. M. Seagraves, The contribution of ultrasonic vocalizations to mouse courtship. *Curr Opin Neurobiol* **38**, 1-5 (2016).
5. K. R. Foster, M. L. Wiederhold, Auditory responses in cats produced by pulsed ultrasound. *The Journal of the Acoustical Society of America* **63**, 1199-1205 (1978).
6. G. Ehret, B. Haack, Ultrasound Recognition in House Mice - Key-Stimulus Configuration and Recognition Mechanism. *J Comp Physiol* **148**, 245-251 (1982).
7. K. Ohyama, J. Kusakari, K. Kawamoto, Ultrasonic Electrocochleography in Guinea-Pig. *Hearing Research* **17**, 143-151 (1985).

8. K. Ohyama, J. Kusakari, K. Kawamoto, Sound perception in the ultrasonic region. *Acta Otolaryngol Suppl* **435**, 73-77 (1987).
9. N. Suga, X. Ma, Multiparametric corticofugal modulation and plasticity in the auditory system. *Nat Rev Neurosci* **4**, 783-794 (2003).
10. J. G. Colebatch, G. M. Halmagyi, N. F. Skuse, Myogenic potentials generated by a click-evoked vestibulocollic reflex. *J Neurol Neurosurg Psychiatry* **57**, 190-197 (1994).
11. H. Ozeki, M. Matsuzaki, T. Murofushi, Vestibular evoked myogenic potentials in patients with bilateral profound hearing loss. *ORL J Otorhinolaryngol Relat Spec* **61**, 80-83 (1999).
12. A. J. Hudspeth, SnapShot: Auditory transduction. *Neuron* **80**, 536 e531 (2013).
13. W. Xiong, Z. Xu, *Mechanotransduction of the Hair Cell*. (Springer Singapore, 2018).
14. B. Coste *et al.*, Piezo1 and Piezo2 are essential components of distinct mechanically activated cation channels. *Science* **330**, 55-60 (2010).
15. L. Wang *et al.*, Structure and mechanogating of the mammalian tactile channel PIEZO2. *Nature*, (2019).
16. B. Xiao, Levering Mechanically Activated Piezo Channels for Potential Pharmacological Intervention. *Annu Rev Pharmacol Toxicol* **60**, 195-218 (2020).
17. M. Beurg, A. C. Goldring, A. J. Ricci, R. Fettiplace, Development and localization of reverse-polarity mechanotransducer channels in cochlear hair cells. *Proc Natl Acad Sci U S A* **113**, 6767-6772 (2016).
18. Z. Wu *et al.*, Mechanosensory hair cells express two molecularly distinct mechanotransduction channels. *Nat Neurosci* **20**, 24-33 (2017).
19. M. Beurg, R. Fettiplace, PIEZO2 as the anomalous mechanotransducer channel in auditory hair cells. *J Physiol* **595**, 7039-7048 (2017).
20. K. P. Hunter, J. F. Willott, Aging and the auditory brainstem response in mice with severe or minimal presbycusis. *Hear Res* **30**, 207-218 (1987).

21. Q. Y. Zheng, K. R. Johnson, L. C. Erway, Assessment of hearing in 80 inbred strains of mice by ABR threshold analyses. *Hear Res* **130**, 94-107 (1999).

22. A. M. Taberner, M. C. Liberman, Response properties of single auditory nerve fibers in the mouse. *J Neurophysiol* **93**, 557-569 (2005).

23. J. A. Garcia-Lazaro, K. N. Shepard, J. A. Miranda, R. C. Liu, N. A. Lesica, An Overrepresentation of High Frequencies in the Mouse Inferior Colliculus Supports the Processing of Ultrasonic Vocalizations. *PLoS One* **10**, e0133251 (2015).

24. J. R. Melcher *et al.*, Generators of the brainstem auditory evoked potential in cat. I. An experimental approach to their identification. *Hear Res* **93**, 1-27 (1996).

25. G. Ehret, Development of absolute auditory thresholds in the house mouse (Mus musculus). *J Am Audiol Soc* **1**, 179-184 (1976).

26. T. Ohyama, A. K. Groves, Generation of Pax2-Cre mice by modification of a Pax2 bacterial artificial chromosome. *Genesis* **38**, 195-199 (2004).

27. H. Yang, X. Xie, M. Deng, X. Chen, L. Gan, Generation and characterization of Atoh1-Cre knock-in mouse line. *Genesis* **48**, 407-413 (2010).

28. A. E. Dubin *et al.*, Inflammatory signals enhance piezo2-mediated mechanosensitive currents. *Cell Rep* **2**, 511-517 (2012).

29. J. Siemens *et al.*, Cadherin 23 is a component of the tip link in hair-cell stereocilia. *Nature* **428**, 950-955 (2004).

30. P. Kazmierczak *et al.*, Cadherin 23 and protocadherin 15 interact to form tip-link filaments in sensory hair cells. *Nature* **449**, 87-91 (2007).

31. B. Pan *et al.*, TMC1 Forms the Pore of Mechanosensory Transduction Channels in Vertebrate Inner Ear Hair Cells. *Neuron* **99**, 736-753.e736 (2018).

32. R. P. Seal *et al.*, Sensorineural deafness and seizures in mice lacking vesicular glutamate transporter 3. *Neuron* **57**, 263-275 (2008).

33. D. Z. He, S. Jia, P. Dallos, Mechanoelectrical transduction of adult outer hair cells studied in a gerbil hemicochlea. *Nature* **429**, 766-770 (2004).

34. R. M. Edge *et al.*, Morphology of the unfixed cochlea. *Hear Res* **124**, 1-16 (1998).

35. C. A. Haselwandter, R. MacKinnon, Piezo's membrane footprint and its contribution to mechanosensitivity. *Elife* **7**, (2018).

36. Y. R. Guo, R. MacKinnon, Structure-based membrane dome mechanism for Piezo mechanosensitivity. *Elife* **6**, (2017).

37. Z. Qiu *et al.*, The Mechanosensitive Ion Channel Piezo1 Significantly Mediates In Vitro Ultrasonic Stimulation of Neurons. *iScience* **21**, 448-457 (2019).

38. A. Edelstein, N. Amodaj, K. Hoover, R. Vale, N. Stuurman, Computer control of microscopes using microManager. *Curr Protoc Mol Biol* **Chapter 14**, Unit14 20 (2010).

39. J. Geng *et al.*, A Plug-and-Latch Mechanism for Gating the Mechanosensitive Piezo Channel. *Neuron*, (2020).

Acknowledgments: We thank Drs Xiaoqin Wang, Xiaoke Chen, Lei Song, Xin Liang, and members of Xiong laboratory for helpful discussions and critical proof-reading of this manuscript, thank the Imaging Core Facility, Technology Center for Protein Sciences at Tsinghua University for assistance of using imaging instruments and software, thank Si Li of Dr. Qingfeng Wu laboratory for help with RNAscope experiment, thank Lili Niu and Xudong Shi of Dr. Hairong Zheng laboratory at Shenzhen Institutes of Advanced Technology, Chinese Academy of Sciences for manufacturing the high-frequency amplifier and ultrasonic transducers, and thank Dr. Qiuying Chen of Dr. Guoxuan Lian laboratory at Institute of Acoustics, Chinese Academy of Sciences for manufacturing the ultrasonic transducers, and thank Dr. Guangzhen Xing at National Institute of Metrology for calibrating the ultrasonic transducers and the high-frequency amplifier. This work was supported by the National Natural

Science Foundation of China (31522025, 31571080, 81873703, 3181101148, and 31825014), Beijing Municipal Science and Technology Commission (Z181100001518001), National Key Scientific Instrument and Equipment Development Project (81527901), and a startup fund from the Tsinghua University-Peking University Joint Center for Life Sciences.

Author contributions: J.L. did the ABR recordings, behavior tests, and data analysis; S.L. did hemicochlear Ca^{2+} imaging and data analysis; C-M.S. did the histology and immunostaining, and maintained the mouse colonies; Q.H. did the immunostaining; Z-K.Z. did the imaging and data analysis; T-T.D. did the Ca^{2+} imaging; L-Z.Z. performed the cochlear culture and injectoporation; S-F.W., C.S., J-F.C., and L.L. conducted the cell culture and molecular experiments; K-X.Y., H-R.Z., Z-Y.L., W-Z.S., B-L.X., and X-W. C. provided materials and designed methods; W.X. supervised the project, designed experiments, generated figures, and wrote the manuscript.

Competing interests: The authors declare no competing interest.

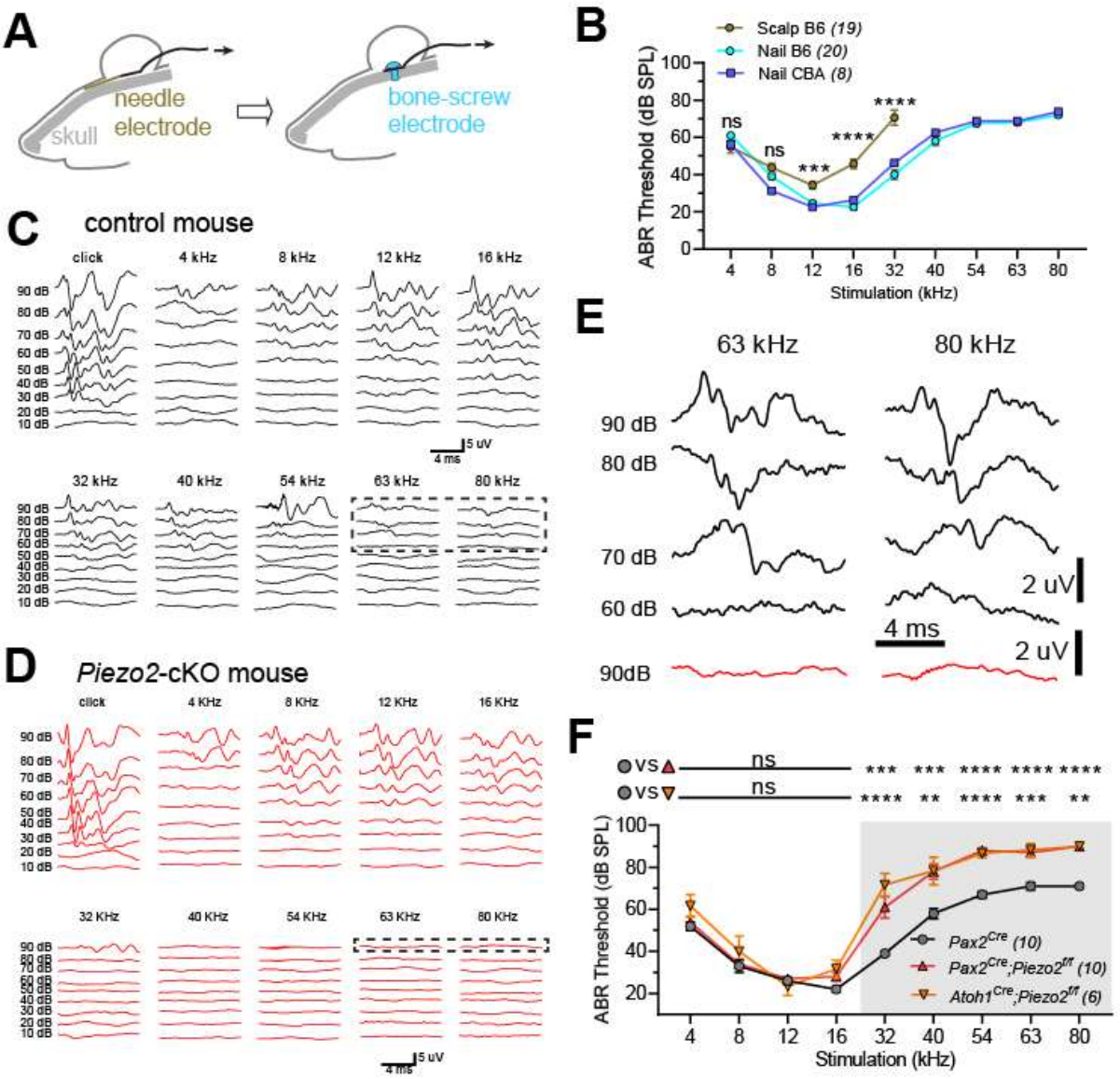

Fig. 1 The mechanosensitive channel Piezo2 is required for ultrasound hearing.

(**A**) Schematic of improved recording configuration of nABR, by which the recording wire was connected with a stainless-steel bone screw implanted on the mouse skull (cyan) comparing to the standard configuration of ABR recording with a needle electrode under scalp (dark yellow) (see fig. S1). (**B**) Comparing to regular ABR in WT C57BL/6J (B6) mice with electrode under scalp (Scalp B6, dark yellow), the nABR achieved an improved sensitivity to ultrasound frequency range in WT B6 mice (Nail B6, grey, including data from Fig. 5a) and CBA/J mice

(Nail CBA, cyan). (**C**-**F**) nABR signals in control *Pax2*^{Cre} mice and *Piezo2*-cKO mice. The inner-ear dependent *Piezo2*-cKO mice were generated by crossing *Piezo2*$^{f/f}$ mice with *Pax2*^{Cre} mice or *Atoh1*^{Cre} mice. Pure-tone sound was played by a TDT EC1 (Coupler Model) electrostatic speaker (up to 80 kHz, the highest frequency can be stably delivered by the speakers). (**C**) Representative example of nABR traces from a control *Pax2*^{Cre} mouse. (**D**) Representative example of nABR traces from a *Pax2*^{Cre}*;Piezo2*$^{f/f}$ mouse. (**E**) Enlarged traces with 63 kHz and 80 kHz sound stimuli framed in (**C**) and (**D**). (**F**) Quantification of pure-tone nABR thresholds in control *Pax2*^{Cre} mice and *Piezo2*-cKO mice. The gray square highlights the distinct ABR threshold of control mice and *Piezo2*-cKO mice upon hearing frequencies within the ultrasound spectrum. All the mice were used at age about 1 month. For (**B**) and (**F**), N numbers are shown in panels; ns, no significance, **p<0.01, ***p<0.001, ****p<0.0001; unpaired *t*-test, error bars, SEM.

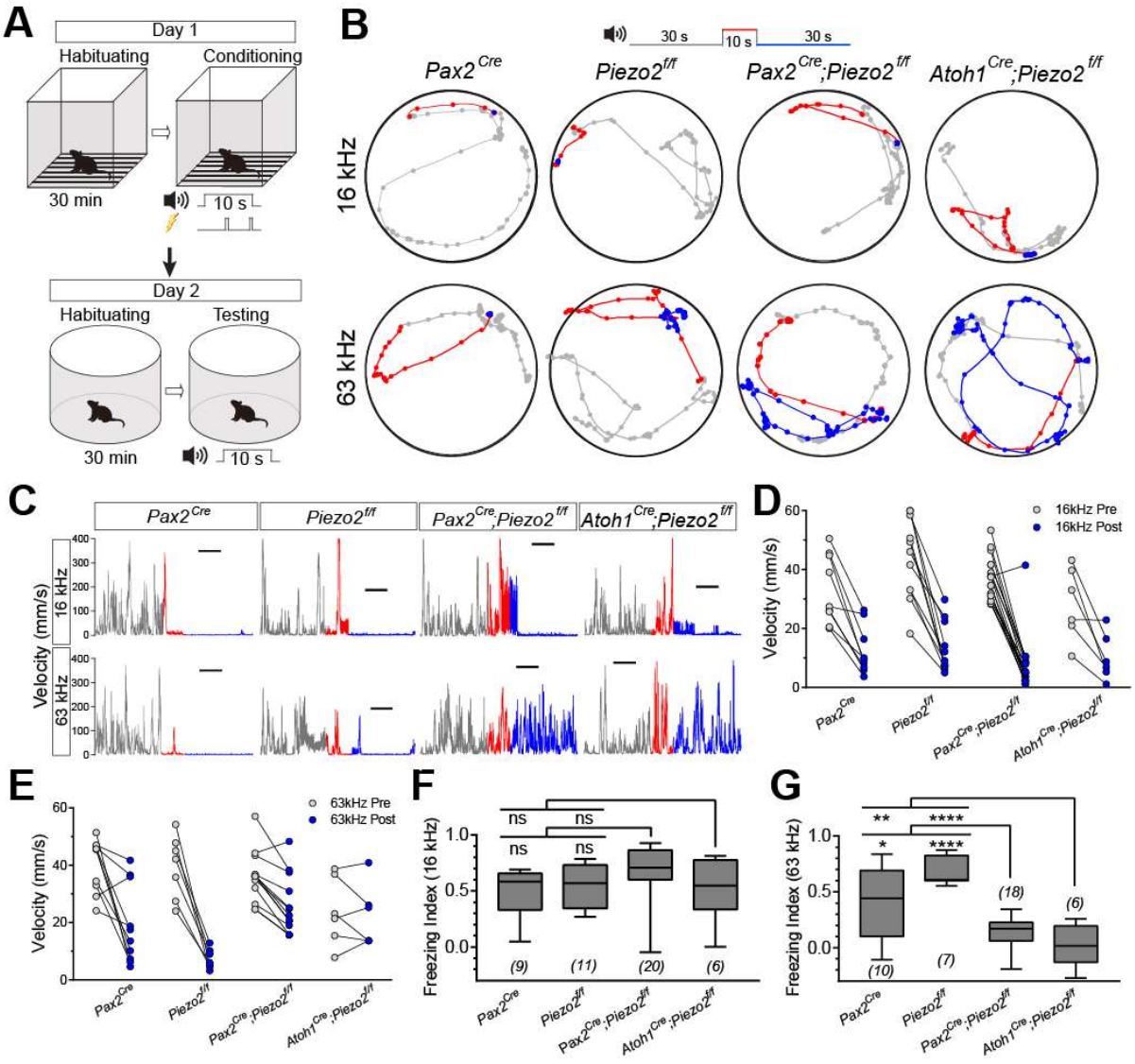

Fig. 2 Ultrasonically-associative freezing behavior is disrupted in *Piezo2*-knockout mice.

(**A**) Sound-cue associated learning of freezing behavior paradigm. Pure-tone sound at 16 kHz or 63 kHz was played by a TDT ES1 (Free Field) electrostatic speaker and was used as the conditional stimulation, and footshock was the unconditional stimulation. (**B**) Representative example of locomotion of control mice and *Piezo2*-cKO mice before (gray, 30 s), during (red, 10 s), and after (blue, 30 s) the pure-tone sound cue at 90 dB SPL. The mice had been trained to pair either 16-kHz cue or 63-kHz cue with the footshock-induced freezing. Dots indicate the

mouse location every 0.5 s. *Pax2*^{Cre} mice and *Piezo2*$^{f/f}$ mice were used as controls. (**C**) Velocity of mice calculated from the locomotion traces in (B). Bar, 10 s. (**D** and **E**) Quantification of averaged velocity in the 30 s before (gray, Pre) and after (blue, Post) 16-kHz cue (C) or 63-kHz cue (D) from data similar to (C). (**F** and **G**) Quantification of freezing index of mice trained and tested with 16-kHz cue (F) or 63-kHz cue (G) calculated from (D) and (E). All the mice were used at age about 1 month. For (F) and (G), N numbers are shown in panels; ns, no significance, *p<0.05, **p<0.01, ****p<0.0001; one-way ANOVA, Box and whiskers, min to max.

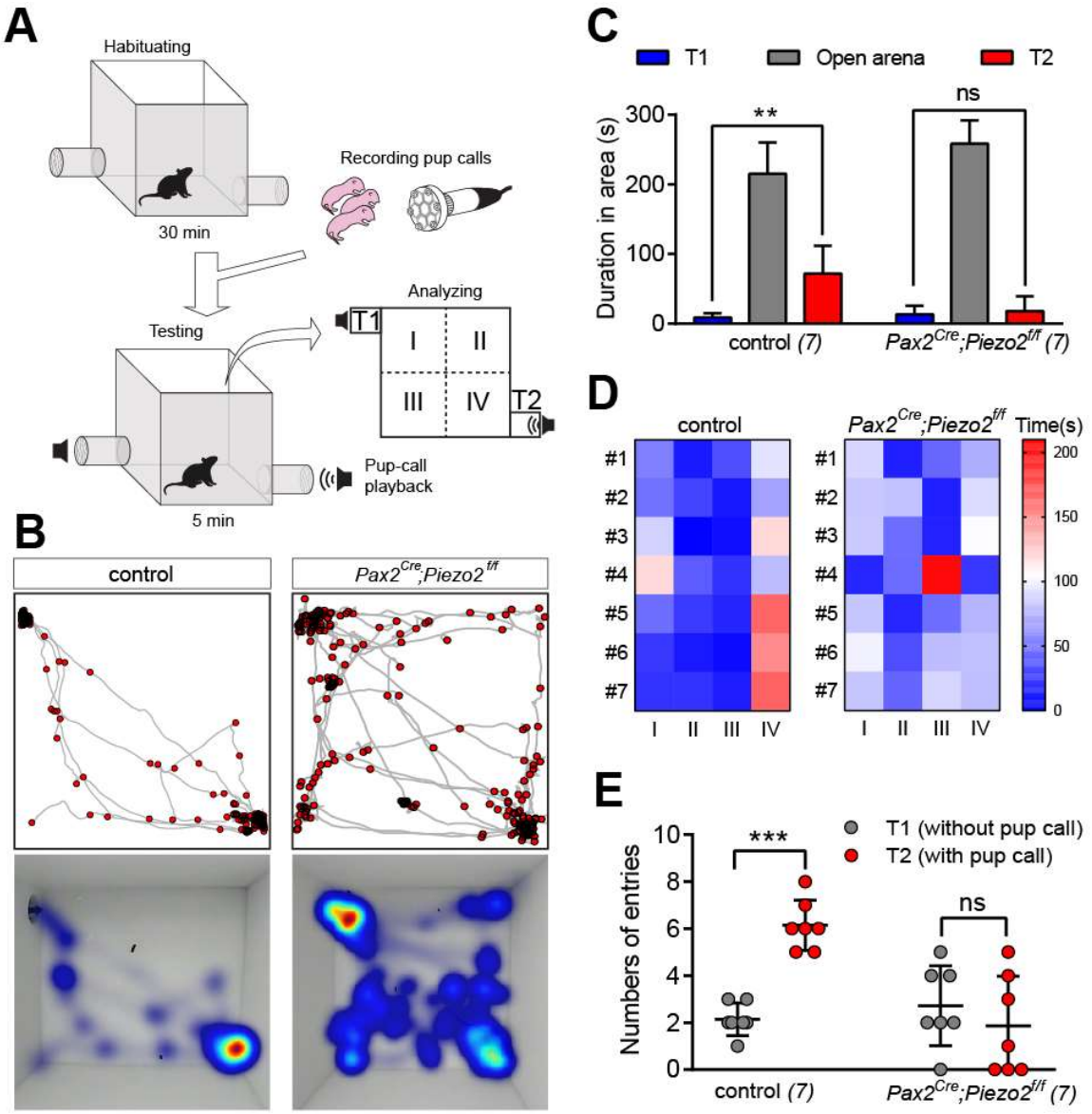

Fig. 3 Pup retrieval behavior is disrupted in *Piezo2*-knockout mice.

(**A**) Schematic of pup retrieval behavior test and analysis. For analysis, the open arena was divided into 4 quadrants and the tubes were named T1 (without playback) and T2 (with playback). (**B**) Representative example of locomotion in 5 min for the control mice and the *Pax2*^{Cre};*Piezo2*$^{f/f}$ cKO mice while hearing the recorded calls of her pups. Upper panels, tracks of mice; lower panels, hot spots of mouse tracks. Dots on tracks indicate the mouse location every 0.5 s. The *Pax2*^{Cre} and *Piezo2*$^{f/f}$ mice were used as control. (**C**) Quantification of duration that

control mice and *Piezo2*-cKO mice stayed in T1, T2, and the open arena during the 5-min playback period. (**D**) Heat map showing the duration spent in each of the 4 quadrants in the open arena by control mice and *Piezo2*-cKO mice. (**E**) Quantification of the numbers of entries into each of the two tubes (with or without pup calls) by control mice and *Piezo2*-cKO mice during the 5-min pup-call playback period. N numbers are shown in panels. For (C) to (E), ns, no significance, **p<0.01, ***p<0.001, paired *t*-test; error bars, SD.

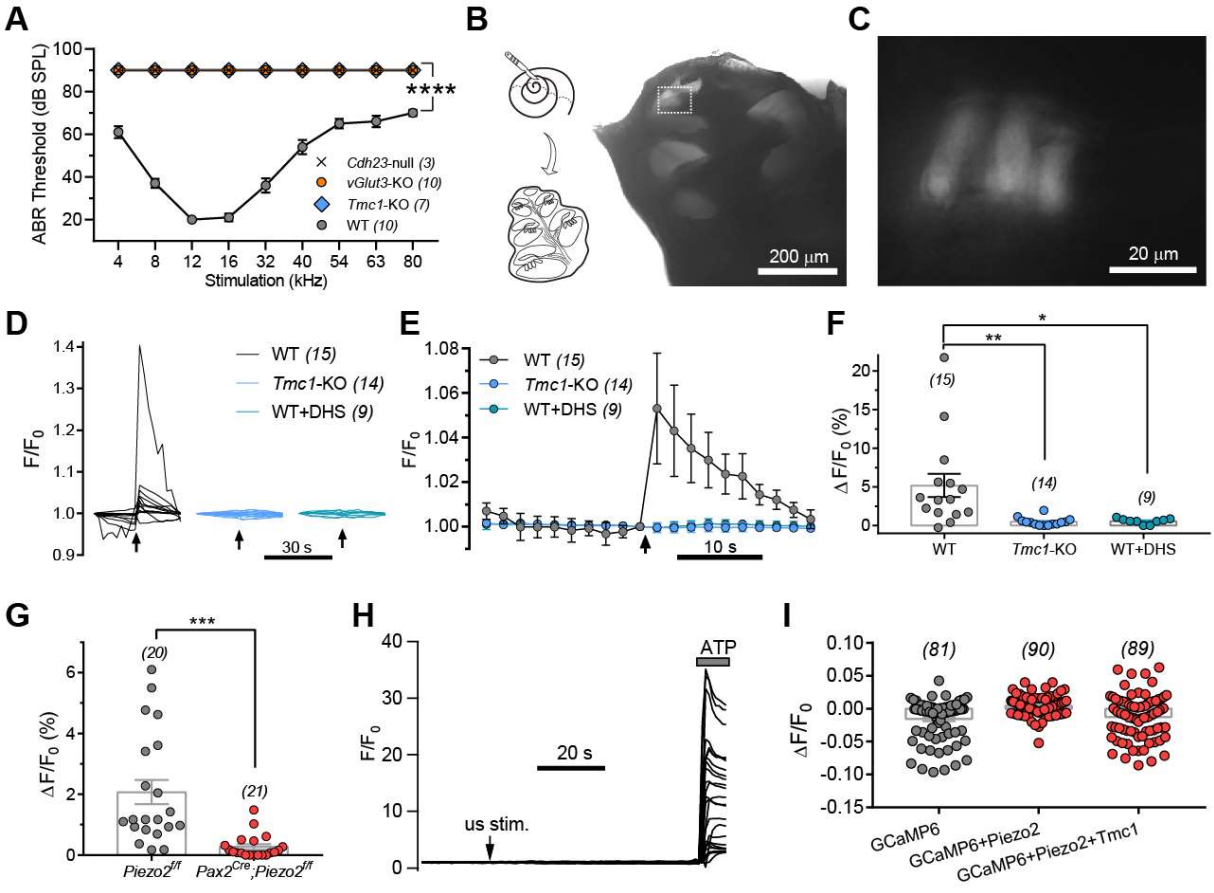

Fig. 4 Hair-cell mechanotransduction is required for ultrasonic hearing.

(**A**) Quantification of pure-tone nABR thresholds of WT mice, *Cdh23*-null mice, *Tmc1*-KO mice, and *vGlut3*-KO mice. (**B**) Left: schematic showing preparation of hemicochlea. Right: a photo of hemicochlea with transmission-light illumination. Bar, 200 μm. (**C**) A fluorescent image showing Fluo-8 AM loaded OHCs, magnified from the apical part (white-dashed frame) of the hemicochlea in (B). Bar, 20 μm. (**D**) Ultrasonic stimulation evoked Ca^{2+} responses of OHCs in hemicochlea preparations. Gray, WT mice; blue grey, *Tmc1*-KO mice; blue green, WT hemicochleae treated with 100 μM DHS. The images were collected every 2 s. (**E**) Averaged Ca^{2+} responses from (D). (**F**) Quantification of peak Ca^{2+} responses of OHCs calculated from recordings in (D). (**G**) Quantification of peak Ca^{2+} responses of OHCs from control *Piezo2*$^{f/f}$ mice and *Pax2*^{Cre};*Piezo2*$^{f/f}$ cKO mice. (**H**) Ultrasonic stimulation failed to evoke Ca^{2+} responses in

HEK293T cells expressing Piezo2. ATP perfusion indicated that the cells had normal Ca^{2+} responsivity. (**I**) Quantification of peak Ca^{2+} responses of HEK293T cells when expressing Piezo2 or Piezo2+Tmc1 from similar recordings in (H). In this figure, all the mice were used at age about 1 month. N numbers are shown in panels. ns, no significance, *p<0.05, **p<0.01, ***p<0.001, ****p<0.0001; For (A) and (G), unpaired *t*-test; For (F), one-way ANOVA; error bars, SEM.

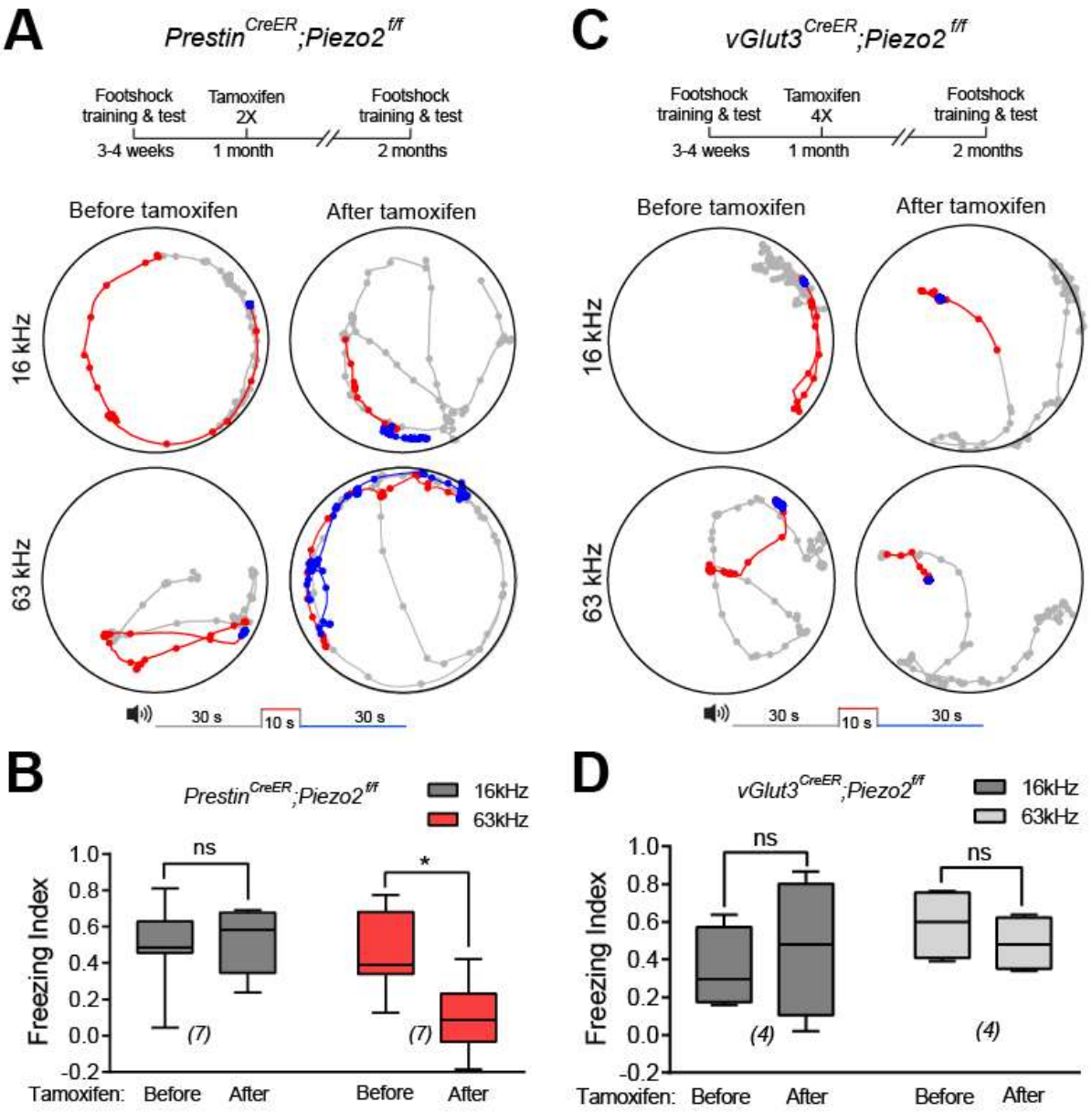

Fig. 5 Mice lack ultrasonic hearing when deleting Piezo2 in outer hair cells.

(**A**) Top: Schematic showing experimental timeline for generation and test of tamoxifen-induced *Prestin*^{CreER};*Piezo2*$^{f/f}$ mice. Bottom: Representative example of locomotion of *Prestin*^{CreER};*Piezo2*$^{f/f}$ mice at 3-4 weeks (before tamoxifen injection) and at 2 months (after tamoxifen injection). Presented was the locomotion before (gray), during (red), and after (blue) the 16-kHz or 63-kHz sound cue. Dots indicate the mouse location every 0.5 s. (**B**)

Quantification of freezing index of *Prestin*^{CreER};*Piezo2*$^{f/f}$ mice trained and tested with 16-kHz cue (dark grey) or 63-kHz (red) cue. (**C**) Top: Schematic showing experimental timeline for generation and test of tamoxifen-induced *vGlut3*^{CreER};*Piezo2*$^{f/f}$ mice. Bottom: Representative example of locomotion of *vGlut3*^{CreER};*Piezo2*$^{f/f}$ mice at 3-4 weeks (before tamoxifen injection) and at 2 months (after tamoxifen injection). (**D**) Quantification of freezing index of *vGlut3*^{CreER};*Piezo2*$^{f/f}$ mice trained and tested with 16-kHz cue (dark grey) or 63-kHz cue (light grey). N numbers are shown in panels. For (**B**) and (**D**), ns, no significance, *p<0.05, ***p<0.001, ****p<0.0001, paired *t*-test; Box and whiskers, min to max.